

Transient MR Signal Changes in Patients with Generalized Tonicoclonic Seizure or Status Epilepticus: Periictal Diffusion-weighted Imaging

Jeong-Ah Kim, Jin Il Chung, Pyeong Ho Yoon, Dong Ik Kim, Tae-Sub Chung, Eun-Ju Kim, and Eun-Kee Jeong

BACKGROUND AND PURPOSE: Our purpose was to investigate transient MR signal changes on periictal MR images of patients with generalized tonicoclonic seizure or status epilepticus and to evaluate the clinical significance of these findings for differential diagnosis and understanding of the pathophysiology of seizure-induced brain changes.

METHODS: Eight patients with MR images that were obtained within 3 days after the onset of generalized tonicoclonic seizure or status epilepticus and that showed seizure-related MR signal changes had their records retrospectively reviewed. T1- and T2-weighted images were obtained of all eight patients. Additional diffusion-weighted images were obtained of five patients during initial examination. After adequate control of the seizure was achieved, follow-up MR imaging was performed. We evaluated the signal changes, location of the lesions, and degree of contrast enhancement on T1- and T2-weighted images and the signal change and apparent diffusion coefficient (ADC) on diffusion-weighted images. We also compared the signal changes of the initial MR images to those of the follow-up MR images.

RESULTS: The initial MR images revealed focally increased T2 signal intensity, swelling, and increased volume of the involved cortical gyrus in all eight patients. The lesions were located in the cortical gray matter or subcortical white matter in seven patients and at the right hippocampus in one. T1-weighted images showed decreased signal intensity at exactly the same location ($n = 6$) and gyral contrast enhancement ($n = 4$). Diffusion-weighted images revealed increased signal intensity at the same location and focally reduced ADC. The ADC values were reduced by 6% to 28% compared with either the normal structure opposite the lesion or normal control. Follow-up MR imaging revealed the complete resolution of the abnormal T2 signal change and swelling in five patients, whereas resolution of the swelling with residual increased T2 signal intensity at the ipsilateral hippocampus was observed in the other two patients. For one of the two patients, hippocampal sclerosis was diagnosed. For the remaining one patient, newly developed increased T2 signal intensity was shown.

CONCLUSION: The MR signal changes that occur after generalized tonicoclonic seizure or status epilepticus are transient increase of signal intensity and swelling at the cortical gray matter, subcortical white matter, or hippocampus on periictal T2-weighted and diffusion-weighted images. These findings reflect transient cytotoxic and vasogenic edema induced by seizure. The reversibility and typical location of lesions can help exclude the epileptogenic structural lesions.

Transient and reversible MR signal changes in patients with generalized tonicoclonic seizure or sta-

tus epilepticus have been reported, and the majority of these reports suggest seizure-induced focal transient cerebral edema as the cause of the transient signal changes (1–4). The experimental status epilepticus models revealed a transient increase of signal intensity and decrease of apparent diffusion coefficient (ADC) on diffusion-weighted images within a few days after the onset of seizure (5–9). Only a few diffusion-weighted imaging studies of patients with epilepsy have been reported to show increased signal intensity on periictal diffusion-weighted images and elevation of ADC in cases of chronic epilepsy (10–13). The transient cerebral abnormalities in patients with epilepsy can be misdiagnosed as tumorous conditions, inflammatory

Received May 18, 2000; accepted after revision October 6.

From the Department of Diagnostic Radiology, the Research Institute of Radiological Science (J.-A.K., J.I.C., P.H.Y., D.I.K., T.-S.C.), and the Division of Medical Science (E.-J.K., E.-K.J.), Yonsei University College of Medicine, Seoul, South Korea.

Presented at the 8th Annual Meeting of the International Society for Magnetic Resonance in Medicine, Denver, 2000.

Address reprint requests to Dong Ik Kim, MD, Department of Diagnostic Radiology, Yonsei University College of Medicine, 134 Shinchon-dong, Seodaemun-ku, 120-752, Seoul, South Korea.

© American Society of Neuroradiology

TABLE 1: Patient profiles

Patient		Seizure Profile			Timing of MR		
No.	Age (y)/ Sex	Type	Duration	EEG	Initial	Follow-up	Clinical Follow-up
1	3/M	CPS (SE)	32 min	Nonfocal	40 hr	9 days, 30 days	SF for 2 mo
2	12/M	GTC	9 min	Nonfocal	46 hr	14 days	SF for 28 mo
3	25/M	CPS	10 min	Left parietotemporal	70 hr	5 mo	SF for 12 mo
4	12/F	GTC	8 min	Left parietotemporal	68 hr	43 days	SF for 18 mo
5	60/M	CPS (SE)	75 min	Right temporal	22 hr	4 mo	SF for 12 mo
6	2/F	CPS (SE)	55 min	Right temporal	44 hr	18 mo	CPS at 6 mo, 12 mo
7	60/F	SPS (SE)	5 days	Left temporal	13 hr	7 days, 4 mo	SPS for 2 mo and then SF for 2 mo
8	51/F	GTC (SE)	3 hr	Nonfocal initially, Right frontotemporal at follow-up	71 hr	26 days	Lost to follow-up

Note.—CPS, complex partial seizure with secondary generalization to generalized tonic clonic seizure without generalization; Duration, total duration of seizure; EEG, location of epileptic discharge on electroencephalography; GTC, generalized tonic clonic seizure; SE, status epilepticus; SF, seizure free; SPS, simple partial seizure; Timing of MRI, timing from seizure onset to MR imaging.

diseases, or demyelinating diseases and may result in unnecessary surgery or invasive biopsy for the patients involved. The purpose of this study was to investigate the transient signal changes on periictal MR images of epileptic patients, to evaluate the clinical significance of these findings for differentiating seizure-induced brain changes from epileptogenic structural lesions, and to understand the pathophysiology of seizure-induced brain changes. We analyzed the signal changes and ADC on periictal diffusion-weighted images and evaluated the significance of diffusion-weighted images for differential diagnosis and for understanding the pathophysiology of seizure-induced structural changes of the brain.

Methods

A retrospective review of 33 patients who underwent cerebral MR imaging during or within 3 days after the onset of generalized tonicoclonic seizure or status epilepticus between February 1998 and June 2000 was conducted. Thirteen patients who displayed clinical evidence of epileptogenic causes, such as systemic hypertension, metabolic imbalance, encephalitis, hypoxic ischemic encephalopathy, or cerebral tumors at initial examination were excluded. Of the remaining 20 patients, eight who satisfied all the following selection criteria were selected: 1) generalized tonicoclonic seizure (primary or secondary generalization of complex partial seizure) or status epilepticus confirmed by EEG with no known underlying epileptogenic causes at initial examination, 2) cerebral MR imaging during the "periictal period" (during or within 3 days after the onset of seizure), 3) focal signal changes noted on periictal MR images, and 4) follow-up MR imaging when there was absent or decreased seizure activity, clinically and electrophysiologically.

The group consisted of four male and four female patients, with ages ranging from 2 to 60 years (mean age, 28 years). Three patients (patients 2, 4, and 8) had generalized tonicoclonic seizures, and four patients (patients 1, 3, 5, and 6) had complex partial seizures with secondary generalization. The remaining patient (patient 7) had a simple partial seizure. Five of the patients (patients 1, 5, 6, 7, and 8) had status epilepticus sustained for >30 minutes (Table 1). MR imaging studies were performed using 1.5-T nuclear MR instruments (GE Signa Advantage; GE Medical systems, Milwaukee, WI). Initial MR

imaging performed during the periictal period included T1-weighted oblique coronal (n = 5) or axial (n = 4) view spin-echo imaging (400/9-10/1 [TR/TE/excitations]; matrix, 256 × 192; section thickness, 7 mm; field of view, 16 × 16 cm), with gadopentetate dimeglumine (Magnevist, Shering, Germany) enhancement at a dose of 0.1 mmol/kg, and T2-weighted oblique coronal view (n = 7) (4000/102/4; matrix, 512 × 256; section thickness, 5 mm; field of view, 16 (16 cm) or axial view (n = 1) (4000/102/1; matrix, 256 × 256; section thickness, 5 mm; section gap, 2 mm; field of view, 16 (16 cm) fast spin-echo imaging. For five patients (patients 2, 5, 6, 7, and 8), diffusion-weighted oblique coronal (n = 1) or axial (n = 5) view imaging (5000/100/1; b = 1000 s/mm; matrix, 128 × 128; section thickness, 5 mm; field of view, 24 (24 cm) and fluid-attenuated inversion recovery (FLAIR) oblique coronal (n = 4) or axial (n = 1) view imaging (11000/127-140/2; inversion time, 2200–2600 ms; matrix, 256 × 192; section thickness, 5 mm; field of view, 16 × 16 cm) were added.

Follow-up MR imaging was performed after adequate seizure control was achieved with the administration of antiepileptic drugs. EEG performed at the time of the follow-up MR imaging showed absent (n = 7) or decreased (n = 1) seizure activity. Follow-up MR imaging was performed 9 days to 18 months after the onset of seizures. In one patient (patient 1), two iterations of follow-up MR imaging were performed after 9 and 30 days, respectively. In seven patients, both T1-weighted contrast-enhanced and T2-weighted imaging were performed, and in two patients (patients 4 and 8), diffusion-weighted and FLAIR imaging were added.

We analyzed the signal change, location of the change, and degree of contrast enhancement on the initial T1- and T2-weighted images and the signal change and ADC of the region of interest on the diffusion-weighted images. The regions of interest were manually drawn on the images. The ADC was determined for regions of interest from ADC mapping by using the following equation:

$$\text{ADC} = \ln(S_0/S_n)/b$$

where S_n is the mean signal intensity for the region of interest and S_0 is the equilibrium intensity for the region of interest on the corresponding T2-weighted image (14). The mean ADC was determined by mean values of ADC_{xx} , ADC_{yy} , and ADC_{zz} . To obtain baseline ADC values, three healthy adult volunteers underwent diffusion-weighted imaging as control participants. The ADC of the region of interest of the lesion was compared with that of the corresponding region of interest in the normal opposite side (patients 5, 6, and 7) or in the control patients (patients 2 and 8). The signal change was di-

TABLE 2: Periictal MR signal changes and single-photon emission CT findings

Patient	Initial MR					Location of MR Signal Change	Location of Increased Perfusion of SPECT
	T2	T1	CE	DWI	FLAIR		
1	+	-	-			Bilateral cingulate gyri	Bilateral superior frontoparietal
2	+	-	-	↑	+	Bilateral cuneus, precuneus	Bilateral parietooccipital
3	+	+	-			Left parietal	
4	+	+	↑			Left frontoparietal	Left frontotemporoparietal
5	+	+	↑↑	↑↑	+	Right parahippocampal, Right uncus, Right occipital	Right temporal, Right parahippocampal
6	+	+	-	↑↑	+	Right hippocampus	
7	+	+	↑	↑↑	+	Left temporal, hippocampal, uncus	Left temporal, Left insular
8	+	+	↑↑	↑↑	+	Bilateral frontotemporal, hippocampal	Bilateral temporal, parietooccipital

Note.—CE, contrast enhancement; DWI, diffusion-weighted image; FLAIR, fluid attenuated inversion recovery; T1, T1-weighted image; T2, T2-weighted image; +, visible signal change; -, no visible signal change; ↑, mild degree of increased signal intensity; ↑↑, high degree of increased signal intensity.

vided into no change, mild change, and marked change by the visual analysis of two radiologists (J.-A.K., J.I.C.). We also compared the findings of the initial and follow-up MR images.

Results

Seizure Profiles and Clinical Data

There was no history of epilepsy among seven patients, and one patient (patient 8) had experienced a complex partial seizure without generalization 6 months before the initial examination. Interictal EEG was performed in five patients (patients 1, 2, 3, 4, and 6) during the periictal period, and ictal EEG was performed in three patients (patients 5, 7, and 8). Periictal EEG showed focal epileptiform discharge in five patients (patients 3, 4, 5, 6, and 7), and nonfocal epileptiform discharge in three patients (patients 1, 2, and 8) (Table 1). In seven patients, epileptic discharge was absent, as revealed by follow-up EEG performed at the time of follow-up MR imaging. In patient 8, follow-up EEG showed subclinical ictal spikes at the right temporal lobe.

Ictal single-photon emission CT (CERASPECT; Digital Scintigraphy, Inc., Waltham, MA) was performed in six patients (patients 1, 2, 4, 5, 7, and 8) with injection of 20 mCi of technetium-99m ethyl cysteine dimer. Ictal single-photon emission CT showed focally increased perfusion at the same hemisphere, including the same lobes of the signal changes of periictal MR imaging for all six patients (Table 2). For four patients (patients 4, 5, 7, and 8), the area of increased perfusion was consistent with the seizure focus revealed by EEG. In patient 8, two iterations of ictal single-photon emission CT were performed 1 day and 11 days after the onset of seizure. Increased perfusion was shown at the bilateral temporal and parietooccipital lobes initially and more localized increased perfusion at the right temporal lobe 11 days after the onset of seizure, which was consistent with the seizure focus revealed by EEG performed at the same time.

Initial MR Imaging

For all eight patients, selected on the basis of seizure-related abnormalities shown on their periictal MR images, MR images revealed focally increased signal intensity, with swelling and increased volume of the involved cortical gyri on T2-weighted images. The lesions were mainly located in the superficial location of the cortical gray matter or subcortical white matter in seven patients, specifically the bilateral cingulate gyri, bilateral parietooccipital, left parietal, left frontoparietal, right temporooccipital lobes including parahippocampal gyrus, left temporal lobe including ipsilateral hippocampus, and bilateral frontotemporal lobes including bilateral hippocampus. In the remaining patient (patient 6), the lesion was located in the right hippocampus (Table 2). Three patients (patients 1, 2, and 8) showed bilateral lesions, whereas three patients (patients 4, 5, and 7) showed ipsilateral multiple lesions.

T1-weighted images revealed decreased signal intensity in the exact same locations in six patients, whereas no significant abnormalities were shown in the other two patients. Gyral contrast enhancement was shown in four patients (patients 4, 5, 7, and 8). The enhancement was mild in patients 4 and 8 and marked in patient 5.

The FLAIR images (n = 5) revealed increased signal intensity with increased volume at the same location, and this was shown more conspicuously than on the T2-weighted images. In patient 5, who witnessed status epilepticus as the initial presentation without known history of seizure, atrophic change of the right hippocampus compared with the left hippocampus was shown (Fig 1).

Periictal Diffusion-weighted Imaging and ADC

All five patients (patients 2, 5, 6, 7, and 8) showed increased signal intensity on diffusion-weighted images in the same locations. Diffusion-weighted images revealed mildly increased signal intensity in the cortical gray matter and subcortical

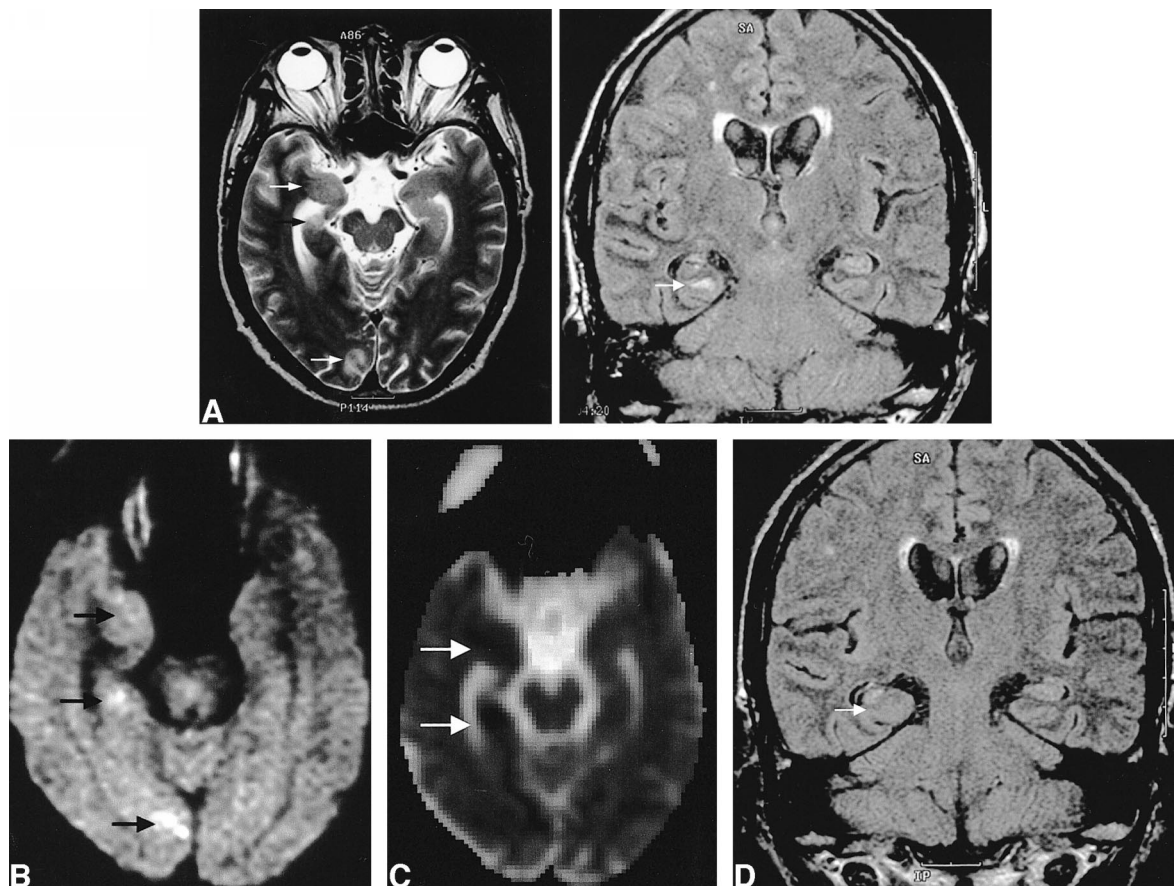


FIG 1. Images of a 60-year-old man (patient 5) with complex partial status epilepticus with secondary generalization as the initial presentation of seizure.

A, Ictal T2-weighted image (*left*) shows increased signal intensity with swelling at the subcortical white matter of the right parahippocampal gyrus, uncus, and occipital cortex (*arrows*). FLAIR image (*right*) shows the increased signal intensity at the parahippocampal gyrus (*arrow*) more conspicuously and the atrophy with increased T2 signal intensity of the body of the right hippocampus, indicating ipsilateral mesial temporal sclerosis.

B, Diffusion-weighted image shows increased signal intensity at exactly the same areas (*arrows*).

C, ADC map shows a 28% decrease of the mean ADC at the right parahippocampal gyrus and a 27% decrease at the uncus (*arrows*).

D, Follow-up FLAIR image obtained 4 months later shows the resolution of the signal change and swelling at the right parahippocampal gyrus (*arrow*) and right mesial temporal sclerosis without remarkable interval change of volume and signal intensity.

white matter of the bilateral cuneus and precuneus in patient 2 (Fig 2). Markedly increased signal intensity was shown at the right parahippocampal gyrus, uncus, and occipital cortex in patient 5 (Fig 1), at the right hippocampus in patient 6 (Fig 3), at the left middle and inferior temporal gyrus, uncus, and ipsilateral hippocampus in patient 7 (Fig 4), and at the left middle, inferior, and superior temporal gyrus, right inferior frontal gyrus, bilateral insular cortex, and bilateral hippocampus in patient 8 (Fig 5).

Consistent with previously published values (15), the measured ADC values in the three normal control participants were $70.2 \pm 2.5 \times 10^{-5} \text{ mm}^2/\text{s}$ in subcortical white matter, $82.1 \pm 2.8 \times 10^{-5} \text{ mm}^2/\text{s}$ in gray matter, $317.7 \pm 4.5 \times 10^{-5} \text{ mm}^2/\text{s}$ in CSF, and $88.9 \pm 1.3 \times 10^{-5} \text{ mm}^2/\text{s}$ in hippocampus. Regions of interest of involved gyrus included cortical gray matter and subcortical white matter. ADC decrease was shown in all five pa-

tients; the decrease of the mean ADC of the region of interest was 8% at the right subcortical white matter of the cuneus and precuneus and 6% at the left in patient 2; 27% at the right uncus, 28% at the right parahippocampal gyrus, and 2% in the occipital cortex in patient 5; 14% at the right hippocampus in patient 6; 19% at the left hippocampus in patient 7; and 9% at the right inferior frontal gyrus, 5% at the right hippocampus, and 8% at the left hippocampus in patient 8 (Table 3). Focally increased ADC was shown in two patients: at the left temporal cortical and subcortical white matter, including the uncus, in patient 7, and at the left inferior temporal gyrus in patient 8 (Table 3).

Follow-up MR Imaging

In patient 1, the follow-up MR image obtained 9 days after the onset of seizure revealed a partial resolution of the signal change on the T2-weighted

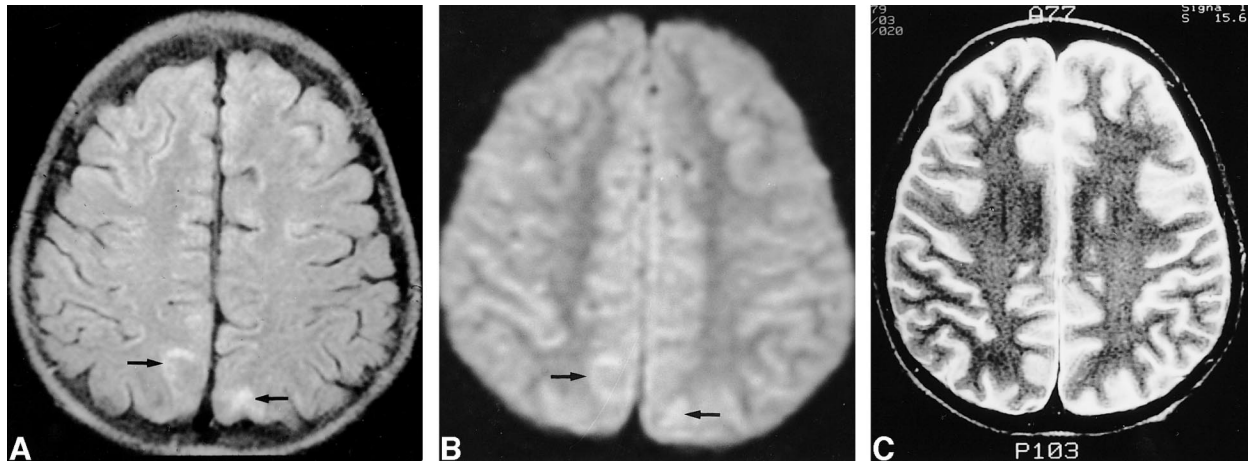


FIG 2. Images of a 12-year-old male patient (patient 2) with generalized tonicoclonic seizure.

A, Initial FLAIR image shows increased signal intensity in the cortical gray matter and subcortical white matter in cuneus and precuneus bilaterally (arrows).

B, Initial diffusion-weighted image shows mildly increased signal intensity in the corresponding areas (arrows). The decrease of the mean ADC was 8% at the right and 6% at the left on the ADC map (not shown).

C, Follow-up T2-weighted image obtained 14 days after the onset of seizure shows complete resolution of the signal change.

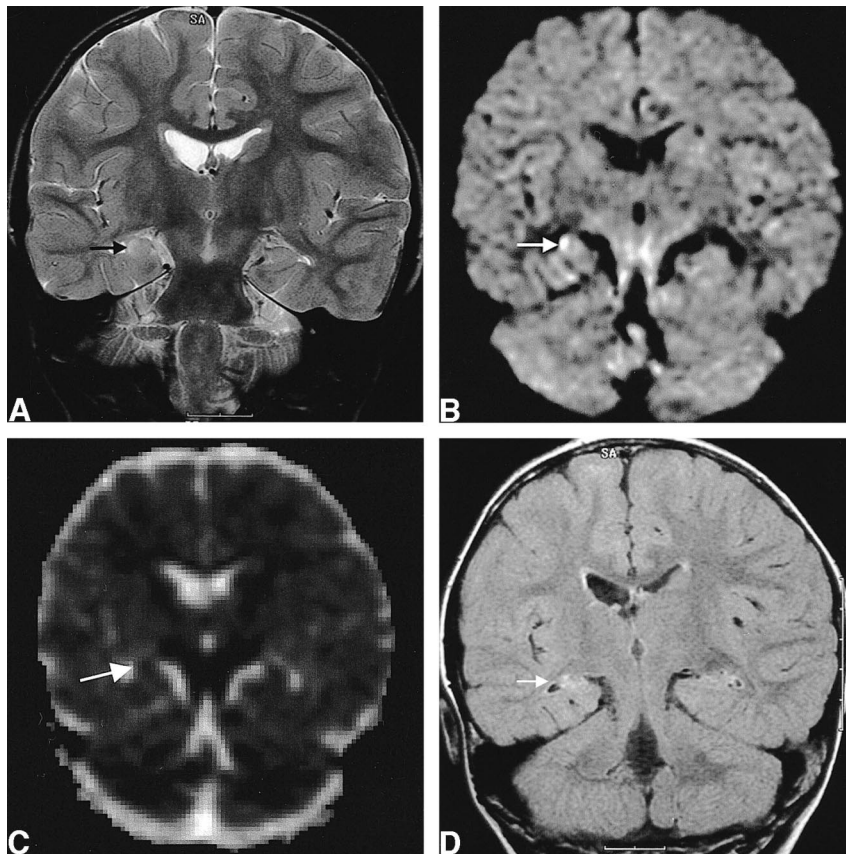


FIG 3. Images of a 2-year-old female patient (patient 6) with complex partial status epilepticus with secondary generalization.

A, Initial T2-weighted image shows increased signal intensity and swelling in the right hippocampus (arrow).

B, Initial diffusion-weighted image shows increased signal intensity in the right hippocampus (arrow).

C, Corresponding ADC map shows 14% decrease of mean ADC (arrow).

D, Follow-up FLAIR image obtained 18 months after the onset of seizure shows the resolution of the swelling and mass effect of the hippocampus (arrow) and increased T2 signal intensity without definite atrophic change of the hippocampus.

image compared with that of the initial T2-weighted image. Complete resolution of the signal change and swelling was observed on the follow-up MR image obtained 30 days after seizure onset (Fig 6). For patient 5, the follow-up MR image obtained 4 months after seizure onset revealed complete resolution of the T2 signal change and swelling at the right parahippocampal gyrus, uncus, and occipital

cortex. The increased signal intensity with atrophic change of the right hippocampus was observed without remarkable interval change of hippocampal volume on FLAIR images (Fig 1). In patient 6, residual increased T2 signal intensity was shown at the right hippocampus on the FLAIR image obtained 18 months after seizure onset, although marked swelling and mass effect resolved (Fig 3).

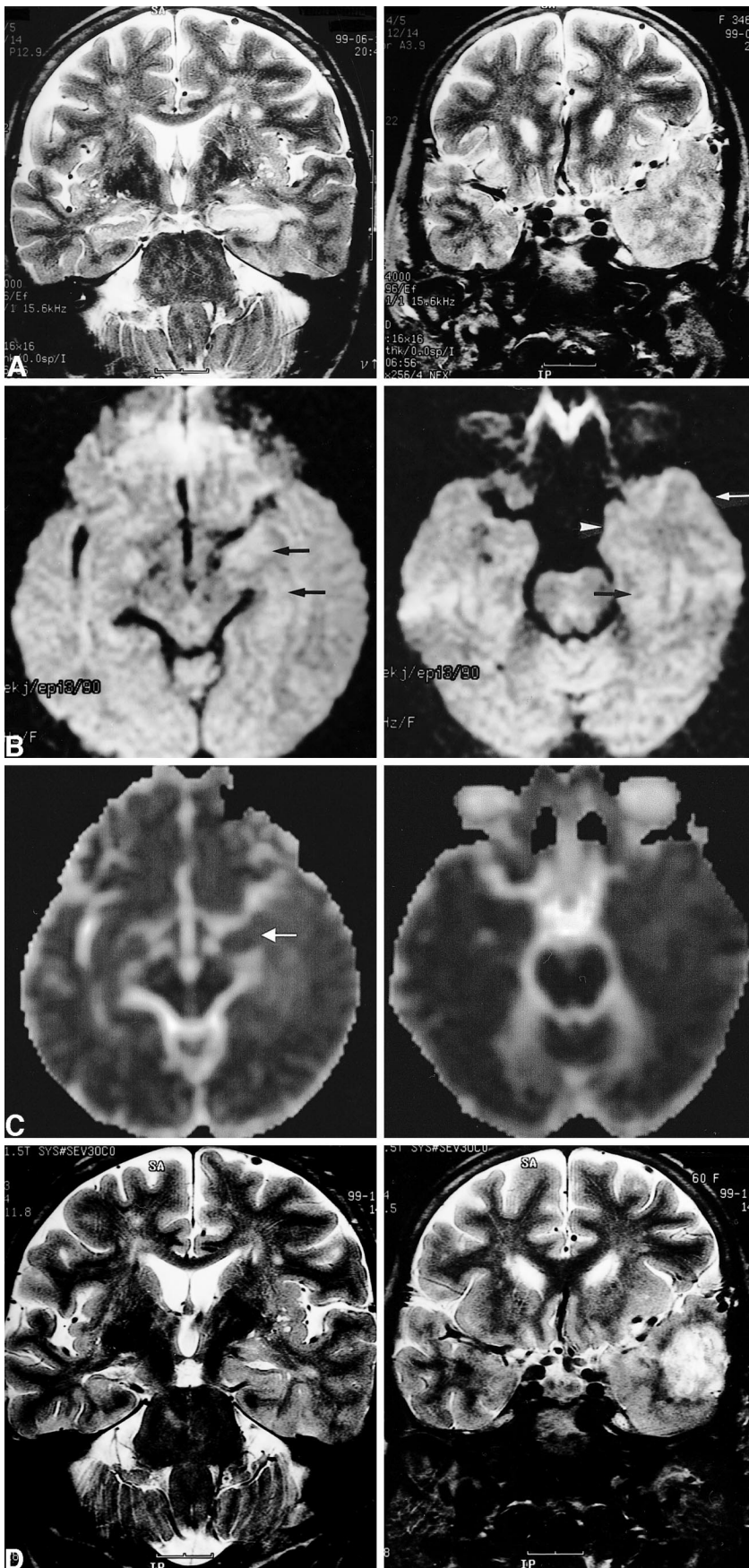


FIG 4. Images of a 60-year-old woman (patient 7) with simple partial status epilepticus sustained for 5 days.

A, Ictal T2-weighted images show extensive swelling and increased signal intensity of the left hippocampus (*left*) and diffuse swelling with increased signal intensity at the cortical gray matter and subcortical white matter of the adjacent left temporal lobe (*right*).

B, Ictal diffusion-weighted images show increased signal intensity and swelling at the left hippocampus (*left, arrows*) and at the uncus (*right, arrowhead*), parahippocampal gyrus (*right, black arrow*), and inferior temporal gyrus (*right, white arrow*).

C, ADC maps show a 19% decrease of the mean ADC at the left hippocampus (*left, arrow*) and a 2% to 5% increase of the mean ADC at the subcortical white matter of the uncus, parahippocampal gyrus, and inferior temporal gyrus (*right*).

D, Follow-up T2-weighted images obtained 4 months after the onset of seizure show the resolution of the marked swelling of the left hippocampus and partial resolution of the increased signal intensity of the left hippocampus (*left*). A tumor was revealed, which was diagnosed as glioblastoma multiforme at the left anterior temporal lobe (*right*). Continued →

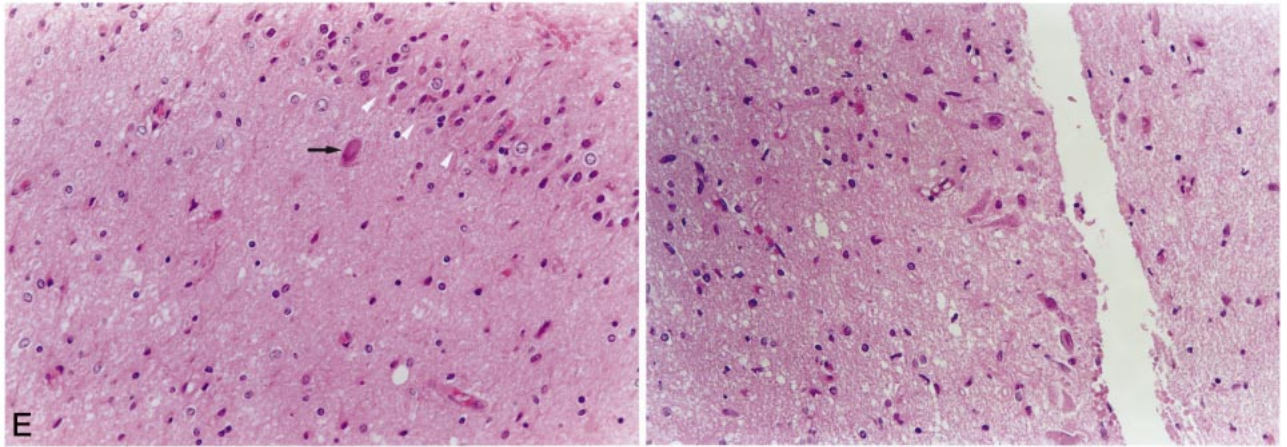


FIG 4. Continued.

E, Light microscopic image of the left hippocampus obtained by amygdalohippocampectomy reveals extensive neuronal loss and gliosis in the CA4 area of the hippocampus (*left*: *arrowheads*, granule cell layer of dentate gyrus; *arrow*, remaining neuron in CA4) and neuronal loss and gliosis in the CA2 area of the hippocampus (*right*). More neurons are preserved in the CA2 area than in the other areas of the hippocampus (CA4, CA3, and CA1).

In patient 7, marked swelling and mass effect of the left hippocampus resolved and partial resolution of diffusely increased T2 signal intensity of the hippocampus was shown (Fig 4). Additionally, a tumor with surrounding edema was shown at the left anterior temporal lobe. In patient 8, multiple increased T2 signal intensity at the left temporal and right frontal gyrus resolved with a slightly atrophic change of the involved gyrus (Fig 5). However, increased T2 signal intensity of the bilateral hippocampus was shown without remarkable change of intensity and volume and newly developed increased T2 signal intensity was shown at the right middle temporal gyrus. Diffusion-weighted and FLAIR images of patient 4 showed a complete resolution of the signal change. Follow-up diffusion-weighted images of patient 8 showed reversal of ADC drop at the right frontal and left temporal gyrus. ADC drop was decreased from 8% to 4% at the left hippocampus but increased from 5% to 10% at the right hippocampus, and a 5% decrease of ADC was newly developed at the right middle temporal gyrus, which was consistent with the seizure focus revealed by follow-up EEG. For the remaining patients, the signal changes resolved completely.

Clinical Follow-up

Seizure control was achieved in six patients during the follow-up period. Patient 6 was initially seizure-free for 6 months, but she later experienced two episodes of complex partial seizure without generalization at 6 and 12 months after follow-up MR imaging, even though she had received anti-epileptic drugs. Patient 7 experienced recurrent simple partial seizures for 2 months, and seizure control was achieved for the next 2 months. Patient 8 did not show any evidence of clinical seizure ac-

tivity, but follow-up EEG revealed subclinical status epilepticus at the right temporal lobe. She was eventually lost to follow-up.

In six patients, the seizure was cryptogenic, and for two patients (patients 7 and 8), the presumed causes of seizure were confirmed during the follow-up examination: brain tumor in patient 7 and multiple sclerosis in patient 8. In patient 7, brain tumor was found at the left temporal lobe 4 months later; anterior temporal lobectomy with ipsilateral amygdalohippocampectomy was performed. The diagnosis was glioblastoma multiforme, and ipsilateral amygdalohippocampectomy revealed neuronal loss and gliosis of CA1, CA2, CA3, and CA4, consistent with hippocampal sclerosis (Fig 4E).

Discussion

Transient MR signal changes in patients with status epilepticus have been reported previously. The signal changes, suggested to be caused by vasogenic or cytotoxic edema, manifested as increased T2 signal intensity in the cortical gray matter or subcortical white matter, with mild mass effects without contrast enhancement (1, 2, 4). Transient contrast enhancement of bilateral mesial temporal cortices in a patient with complex partial status epilepticus was previously reported, which suggested that the enhancement was induced by focally increased perfusion owing to increased metabolism at the epileptogenic area, resulting in an increased consumption of oxygen, hypoxia, hypercarbia, lactic acidosis, and vasodilation (3). The transient increase of T2 signal intensity in the temporal subcortical white matter and gray matter was reported in a patient with partial status epilepticus (4). It was suggested that the changes in the white matter were because of vasogenic edema induced by focally increased perfusion and vascular permeability,

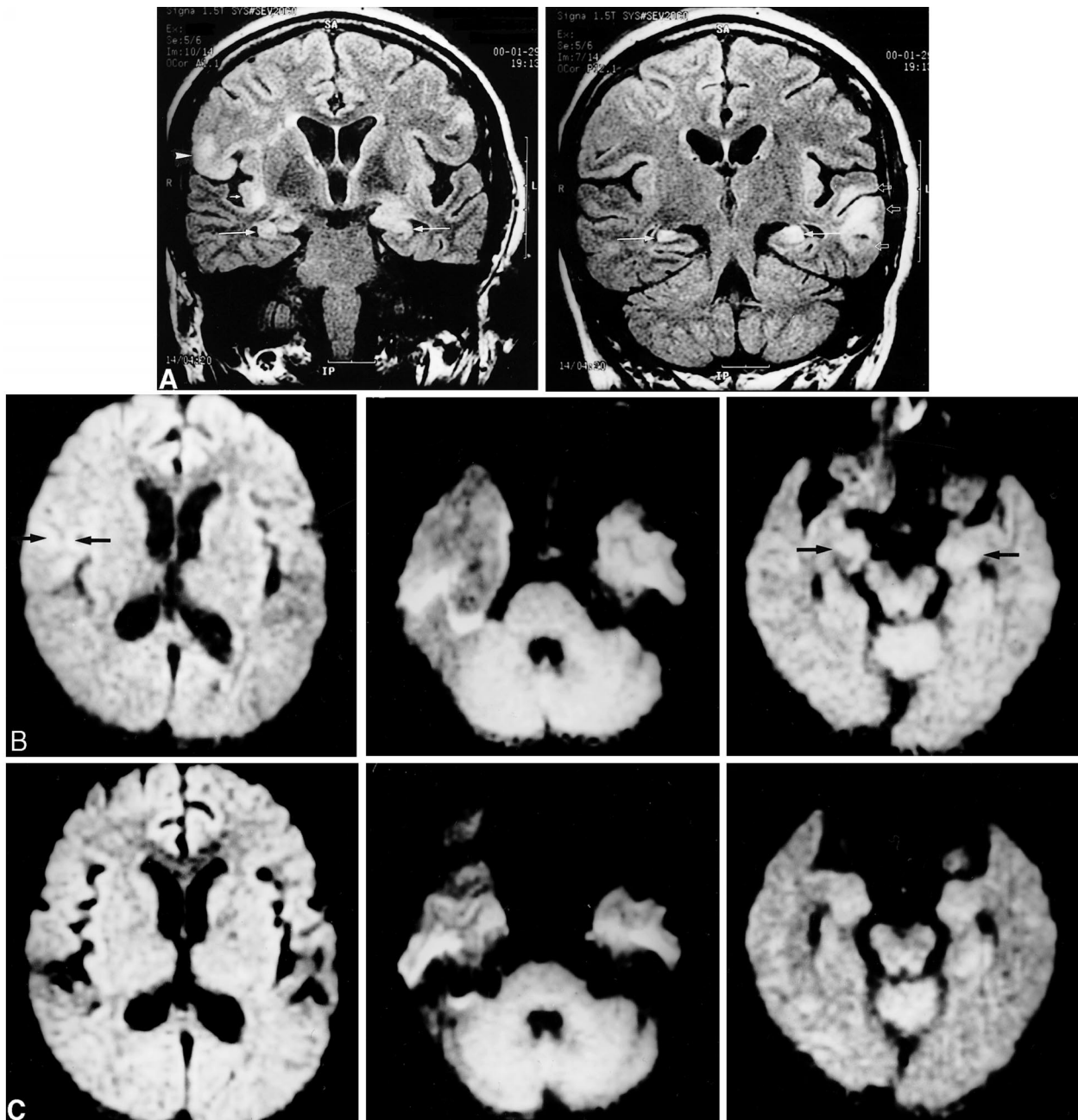


FIG 5. Images of a 51-year-old woman (patient 8) with generalized tonicoclonic status epilepticus.

A, Initial FLAIR images show multiple increased signal intensity and swelling at the cortical gray matter and subcortical white matter of the right inferior frontal gyrus (*left, arrowhead*), right insular cortex (*left, short arrow*), left superior, middle, and inferior temporal gyri (*right, open arrows*), and bilateral hippocampi (*long arrows*).

B, Initial diffusion-weighted images show increased signal intensity at the right inferior frontal gyrus (*left, arrows*), left temporal lobe (*middle*), and bilateral hippocampi (*right, arrows*).

C, Follow-up diffusion-weighted images show resolution of the signal changes of the right frontal (*left*) and left temporal (*middle*) lobe. The increased signal intensity at the bilateral hippocampi did not resolve (*right*).

whereas the gray matter change was because of cytotoxic edema induced by focal ischemia or other metabolic abnormalities. It was further suggested that the possibility of associated neoplasm could not be excluded if the signal change did not resolve on follow-up MR images. Cox et al (1) reported a case in which a reversible increase of T2 signal intensity and mass effect were shown at the right hippocampus. They suggested that these findings

were the result of vasogenic and cytotoxic edema induced by seizures and suggested it as a possible first step in the development of mesial temporal sclerosis.

In this study, the signal changes shown on perirhinal MR images were primarily confined to the superficial location of cortical gray matter, subcortical white matter, or hippocampus. These changes were shown on both T2-weighted and FLAIR im-

TABLE 3: Apparent diffusion coefficient of region of interest

Patient	Location of Region of Interest	Mean ADC (SD)		
		Right	Left	Ratio of Lesion to Normal of Mean ADC
2	Bilateral cuneus and precuneus	66.4 (1.8)	68.2 (1.4)	Right 0.92, Left 0.94
5	Right parahippocampal	60.6 (1.1)	84.2 (1.6)	0.72
	Right uncus	60.5 (1.6)	82.9 (2.3)	0.73
	Right occipital	76.9 (1.0)	78.2 (0.9)	0.98
6	Right hippocampus	77.6 (2.7)	90.2 (2.1)	0.86
7	Left temporal	81.3 (2.1)	86.1 (2.4)	1.05
	Left hippocampal	89.9 (2.1)	72.8 (2.9)	0.81
	Left uncus	81.4 (2.2)	83.0 (1.9)	1.02
8	Left inferior temporal	1:77.4 (1.9)	79.0 (1.6)	1.02
		2:77.9 (1.1)	81.0 (1.1)	1.04
	Right middle temporal	1: 77.6 (0.7)	78.1 (0.9)	0.99
		2: 73.1 (0.6)	77.8 (0.8)	0.94
	Right inferior frontal	1:74.6 (1.4)	82.0 (1.2)	0.91
		2:81.0 (1.1)	81.8 (0.9)	0.99
	Bilateral hippocampal	1:84.2 (1.7)	81.4 (2.2)	Right 0.95, Left 0.92
2:80.3 (1.5)		85.7 (1.9)	Right 0.9, Left 0.96	

Note.—Mean ADC, mean ADC of ADCxx, ADCyy and ADCzz ($\times 10^{-5}$ mm²/S); In patient 8, 1 means initial and 2 means follow-up values.

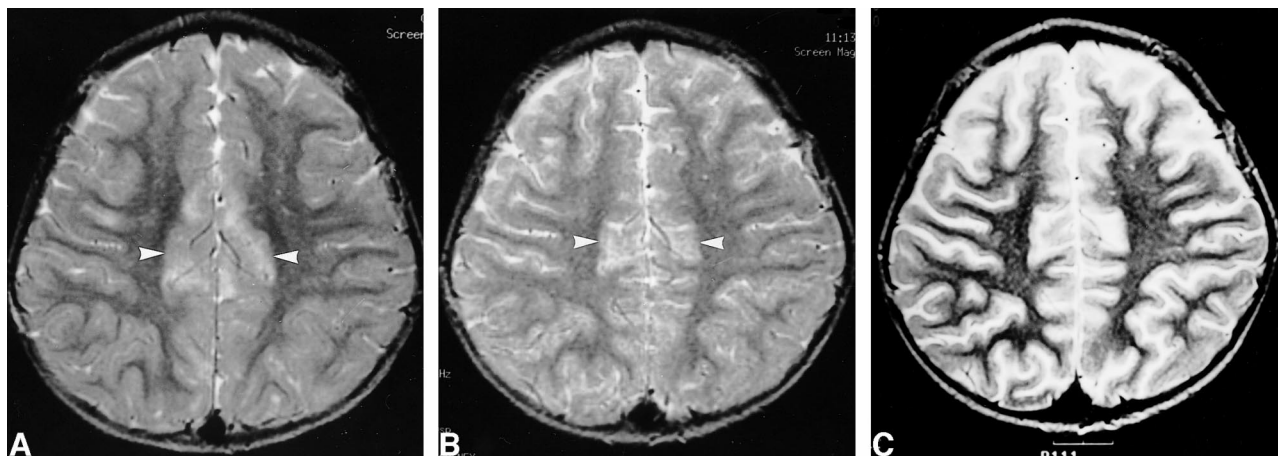


FIG 6. Images of a 3-year-old male patient (patient 1) with complex partial status epilepticus show the resolution process of the signal change.

- A, Initial T2-weighted image shows increased signal intensity in the cortical gray matter of bilateral cingulate gyri (arrows).
 B, Follow-up T2-weighted image shows partial resolution of the signal intensity 9 days after seizure onset.
 C, Follow-up T2-weighted image shows complete resolution of the signal intensity 30 days after seizure onset.

ages, with FLAIR images showing the changes more conspicuously, as reported in previous studies (16–18).

Diffusion-weighted imaging studies of experimentally induced status epilepticus in rats have been reported. Diffusion-weighted imaging reveals an acute postictal depression of ADC, interictal normalization, and then chronic elevation in the seizure focus (6–9). In an experimental complex partial status epilepticus model induced by kainic acid injection, the ADC showed a decrease of 9% to 20% and 36% to 49% compared with the baseline level at 3 and 24 hours after injection, respectively, with normalization thereafter (9). Nakasu et al (8) reported a significant increase of signal intensity on diffusion-weighted images at the bilateral amygdala and pyriform cortices in rats, with

seizure sustained for 1 hour without discernible signal changes seen on T2-weighted images. They suggested that diffusion-weighted imaging could be a useful method for investigating the mechanism of seizure-induced brain damage. Zhong et al (7) suggested that diffusion-weighted imaging might be useful for mapping recent intense seizure activity in human patients with intractable epilepsy.

The changes on the diffusion-weighted images in cases of epilepsy are similar to the findings of early cerebral ischemia; however, the mechanisms resulting in these findings may be different from that of ischemia. With ischemia, the cerebral blood flow decreases, resulting in subsequent glucose metabolic imbalance, impaired pump activity with increased permeability of cell membranes, and cell necrosis. However, with epilepsy, glucose levels

and oxygen metabolisms in brain cells increase, resulting in increased cerebral blood flow; if the compensatory increase of blood flow is not sufficient, anaerobic metabolisms may take over, resulting in excess production of lactic acid and decrease of phosphocreatine. With status epilepticus, the metabolism is markedly increased, resulting in depletion of adenosine triphosphate and energy reserves at its later stage. Inevitably, this will result in impaired ion exchange pump functions and increased membrane ion permeability of the cells, resulting in the increase of extracellular potassium ion concentration and accumulation of intracellular calcium ion together with swelling of neuronal and glial cells, consistent with findings observed in cytotoxic edema. The intracellular calcium accumulation causes cell death, possibly by activating many Ca^{2+} -dependent enzymes, such as proteases and phospholipases, which can lead to cell membrane breakdown (5, 19). The change of ADC in cases of epilepsy reflects cell damage induced by seizure activities and not by hypoxia or cerebral ischemia (5).

Only a few cases showing changes on periictal diffusion-weighted images of epileptic patients have been reported (10, 11). Wiesmann et al (10) showed a transiently increased signal change on diffusion-weighted images of a patient with focal motor status epilepticus. In one reported case of focal motor status epilepticus, the concordance of the area of focal electrocorticographic seizure activity with the area of signal changes on the periictal diffusion-weighted image was shown (11). This suggested the potential usefulness of periictal diffusion-weighted imaging as a noninvasive technique for the localization of ictal focus. Interictal diffusion-weighted imaging studies have shown an increase of ADC of the hippocampus in patients with mesial temporal sclerosis and have implied that the interictally increased ADC represents an epileptogenic region with neuronal loss, gliosis, and expanded extracellular space (12, 13).

In the present study, periictal diffusion-weighted images of five patients showed increased signal intensity at the cortical gray matter and subcortical white matter at the same area as that on the T2-weighted and FLAIR images. The areas of signal changes on the periictal diffusion-weighted images were located in the same lobes with the seizure foci noted on the EEG and ictal single-photon emission CT scans of all five patients. Some showed decreased ADC, reflecting the seizure-related cytotoxic edema, although this was not pathologically proved, and some showed focally increased ADC by 2% to 5% in two patients. Linear correlation of increase of ADC and extracellular water volume was shown in cat brains, suggesting that diffusion mapping could differentiate between the vasogenic and cytotoxic edema (20). Nedelcu et al (21) reported biphasic evolution of brain edema in rats with hypoxic ischemic injury consisting of early neuronal cytotoxic and late glial vasogenic edema.

Although the pathophysiology and temporal evolution of seizure-related brain edema are different from those of ischemia, the ADC may depend on the temporal evolution of edema and the timing of measurement. Zhong et al (7) reported linear correlation of degree of ADC reduction with the duration of flurothyl administration and suggested that diffusion-weighted imaging might be useful for mapping recent intense seizure activity in human patients with intractable epilepsy. The duration of seizure activity and ADC drop did not correlate well in this study, but definitive comparison was impossible because the timing of ADC measurement, seizure type, and intensity were variable among the patients.

It was previously reported that tissues with decreased ADC of >10% to 15% at 12 hours became necrotic, whereas tissues with decreased ADC of 10% recovered in ischemic rat models (21). Concordant with this report, our study showed a 10% decrease of ADC in two patients, and their follow-up MR images showed complete or partial resolution of the signal changes; follow-up diffusion-weighted imaging was performed in only one of the two patients (patient 8), and it showed the partial resolution of the ADC drop at the left hemisphere and newly developed ADC decrease at the right hemisphere that was consistent with ictal focus on follow-up EEG. Significant ADC decrease of >10% was noted in three patients (patients 5, 6, and 7) at the mesial temporal cortex. Patient 5, who initially presented with status epilepticus, had ipsilateral hippocampal atrophy revealed by initial MR imaging, with markedly decreased ADC shown at the parahippocampal gyrus. Subsequently, the increased T2 signal intensity of parahippocampal gyrus resolved on the follow-up images and the patient remained seizure-free for 12 months during the follow-up period. For the remaining two patients, increased T2 signal intensity at the ipsilateral hippocampus did not resolve without definite atrophic change, although the swelling and mass effect resolved, and they continued to suffer from partial seizure disorder during the follow-up period. Patient 7, whose images showed extensive swelling with increased T2 signal intensity and a 19% decrease of ADC at the left hippocampus, was diagnosed with ipsilateral hippocampal sclerosis 4 months after seizure onset; however, the hippocampus did not show definitive atrophic change on follow-up MR images obtained at that time. The presumed cause of the status epilepticus in patient 7 was glioblastoma multiforme; however, it was clearly shown that prolonged status epilepticus-induced cytotoxic and vasogenic edema at hippocampus progressed to ipsilateral hippocampal sclerosis in the relatively short period of 4 months. It is suggested that cytotoxic edema at the hippocampus induced by prolonged status epilepticus may be the first step in the development of seizure-induced brain damage progressing to hippocampal sclerosis. Wiesmann et al (13) reported elevation of ADC

and prolonged T2 relaxation time in two hippocampi with normal volume in patients with hippocampal sclerosis and suggested that prolonged T2 relaxation time reflected damage on the microstructural level in those hippocampi and that ADC or T2 measurement may possibly be more sensitive in detecting hippocampal sclerosis. A case was reported that showed the development of hippocampal sclerosis in an adult patient with generalized tonicoclonic seizure in which MR imaging performed 14 days after seizure onset revealed increased T2 signal intensity of right hippocampus with symmetrical hippocampal volumes and severe atrophy of that hippocampus 8 months later (22). Increased T2 signal intensity without definite atrophic change of ipsilateral hippocampus was shown on the follow-up MR images of patient 6, who developed refractory complex partial seizure, but hippocampal sclerosis was not confirmed. However, it is expected that long-term follow-up MR imaging could possibly reveal the atrophy of the hippocampus.

Several cases showing the development of hippocampal atrophy after status epilepticus have been reported (23–26). In the acute stage of status epilepticus in humans, neuropathologic examinations reveal visibly swollen hippocampi with extensively destroyed neuron, and in the chronic stage, they reveal shrunken hippocampi with chronic gliosis (27). Neuropathologic examination of the hippocampus in a patient with status epilepticus showed acutely reactive astrocytes with swollen cytoplasm and neuropil, consistent with cytotoxic edema; the reversible signal abnormality of hippocampus in this patient reflected reversible cytotoxic edema (24).

Hippocampal sclerosis is characterized by neuronal loss and gliosis, particularly affecting the pyramidal neurons of CA1, CA3, and CA4 pathologically (28). The pathogenesis of hippocampal sclerosis is debatable; however, childhood toxic events (such as febrile convulsion or hypoxia) or excitotoxins (such as glutamate or aspartate) are possible causes of hippocampal sclerosis (28–31). Hippocampal neuronal loss can be induced in animals by seizure activity (31–33). The excitotoxicity is an important mechanism of the neuronal damage in the hippocampus because excess glutamate release occurs in seizure, leading to calcium influx due to its action on *N*-methyl-D-aspartate receptors, resulting in subsequent cell deaths (31). It was shown that the region of hippocampus (CA1, CA4) of a patient with hippocampal sclerosis had high density of *N*-methyl-D-aspartate receptors (22). Bouilleret et al (30) showed that mesial temporal sclerosis developed by excitotoxic lesion of intra-hippocampal kainate injection in mice. To our knowledge, this study is the first of its kind to show the subsequent development of hippocampal sclerosis in a patient presenting with status epilepticus as the first manifestation of seizure and showing increased signal intensity with a decrease of ADC

at the hippocampus on periictal diffusion-weighted images. The long-term follow-up of patients whose periictal diffusion-weighted images had focal high signal intensity is needed to determine the possibility of subsequent development of hippocampal sclerosis or other structural damages of the brain. It is possible that the reversibility of the signal changes and the characteristic locations of cortical or subcortical white matter or hippocampus on periictal MR images can be used as diagnostic clues to exclude epileptogenic lesions such as neoplasm, inflammatory lesions, or demyelinating lesions and to avoid unnecessary invasive procedures resulting from misdiagnosis.

This study was limited in that only five patients underwent periictal diffusion-weighted imaging and only one patient underwent follow-up diffusion-weighted imaging. However, the findings on periictal MR and diffusion-weighted images in this study reflect that seizure-induced cytotoxic and vasogenic edema manifests as transient signal changes and may be useful in understanding the pathophysiology of seizure-induced brain damage in patients with epilepsy.

In conclusion, the transient MR signal changes for patients with generalized tonicoclonic seizure or status epilepticus are a transient increase of signal intensity and swelling at the cortical gray matter, subcortical white matter, or hippocampus on periictal T2-weighted and diffusion-weighted images. These findings reflect transient cytotoxic and vasogenic edema induced by seizure, although this has not been proven pathologically. The reversibility and characteristic locations of the signal changes may help exclude the possibility of epileptogenic structural lesions. The case of status epilepticus progressing to hippocampal sclerosis suggests that prolonged seizure-induced cytotoxic and vasogenic edema of the hippocampus is an initial step in brain damage progressing to hippocampal sclerosis, and periictal diffusion-weighted imaging may be a non-invasive diagnostic tool useful for localization of seizure-induced brain damage.

References

1. Cox JE, Mathews VP, Santos CC, Elster AD. **Seizure-induced transient hippocampal abnormalities on MR: correlation with positron emission tomography and electroencephalography.** *AJNR Am J Neuroradiol* 1995;16:1736–1738
2. Kramer RE, Luders H, Lesser RP, et al. **Transient focal abnormalities of neuroimaging studies during focal status epilepticus.** *Epilepsia* 1987;28:528–532
3. Horowitz SW, Merchut M, Fine M, Azar-Kia B. **Complex partial seizure-induced transient MR enhancement.** *J Comput Assist Tomogr* 1992;16:814–816
4. Henry TR, Drury I, Brunberg JA, Pennell PB, McKeever PE, Beydoun A. **Focal cerebral magnetic resonance changes associated with partial status epilepticus.** *Epilepsia* 1994;35:35–41
5. Helerper JA, Huang N. **Diffusion-weighted imaging in epilepsy.** *Magn Reson Imaging* 1995;13:1227–1231
6. Zhong J, Petroff OA, Prichard JW, Gore JC. **Changes in water diffusion and relaxation properties of rat cerebrum during status epilepticus.** *Magn Reson Med* 1993;30:241–246
7. Zhong J, Petroff OA, Prichard JW, Gore JC. **Barbiturate-reversible reduction of water diffusion coefficient in flurothyl-in-**

- duced status epilepticus in rats. *Magn Reson Med* 1995;33:253-256
8. Nakasu Y, Nakasu S, Uremura S, Inubushi T, Handa J. Diffusion-weighted MR in experimental sustained seizures elicited with kainic acid. *AJNR Am J Neuroradiol* 1995;16:1185-1192
 9. Righini A, Pierpaoli C, Alger JR, Chiro GD. Brain parenchyma apparent diffusion coefficient alterations associated with experimental complex partial status epilepticus. *Magn Reson Imaging* 1994;12:865-871
 10. Wieshmann UC, Symms MR, Shorvon SD. Diffusion changes in status epilepticus. *Lancet* 1997;350:493-494
 11. Diehl B, Najm I, Ruggieri P, et al. Periictal diffusion-weighted imaging in a case of lesional epilepsy. *Epilepsia* 1999;40:1667-1671
 12. Hugg JW, Butterworth EJ, Kuzniecky RI. Diffusion mapping applied to mesial temporal lobe epilepsy. *Neurology* 1999;53:173-176
 13. Wieshmann UC, Clark CA, Symms MR, Barker GJ, Bimie KD, Shorvon SD. Water diffusion in the human hippocampus in epilepsy. *Magn Reson Imag* 1999;17:29-36
 14. Moseley ME, Cohen Y, Kucharczyk J, et al. Diffusion-weighted MR imaging of anisotropic water diffusion in cat central nervous system. *Radiology* 1990;176:439-445
 15. Pierpaoli C, Jezzard P, Basser PJ, Bamett A, Chiro GD. Diffusion tensor MR imaging of the human brain. *Radiology* 1996;201:637-648
 16. Bergin PS, Fish DR, Shorvon SD, Oatridge A, deSouza NM, Bydder GM. Magnetic resonance imaging in partial epilepsy additional abnormalities shown with the fluid attenuated inversion recovery (FLAIR) pulse sequence. *J Neurol Neurosurg Psychiatry* 1995;58:439-443
 17. Jack CR Jr, Rydberg CH, Kreke KN, et al. Mesial temporal sclerosis: diagnosis with fluid-attenuated inversion-recovery versus spin-echo MR imaging. *Radiology* 1996;199:367-373
 18. Wieshmann UC, Free SL, Everitt AD, et al. Magnetic resonance imaging in epilepsy with a fast FLAIR sequence. *J Neurol Neurosurg Psychiatry* 1996;61:357-361
 19. Wasterlain CG, Fujikawa DG, Penix LR, Sankar R. Pathophysiologic mechanisms of brain damage from status epilepticus. *Epilepsia* 1993;34:S37-S53
 20. Kuroiwa T, Nagaoka T, Ueki M, et al. Correlation between the apparent diffusion coefficient, water content, and ultrastructure after induction of vasogenic brain edema in cats. *J Neurosurg* 1999;90:499-503
 21. Nedelcu J, Klein MA, Aguzzi A, Boesiger P, Martin E. Biphasic edema after hypoxic-ischemic brain injury in neonatal rats reflects early neuronal and late glial damage. *Pediatr Res* 1999;46:297-304
 22. Jackson GD, Chambers BR, Berkovic SF. Hippocampal sclerosis: development in adult life. *Dev Neurosci* 1999;21:207-214
 23. Tien RD, Felsberg GJ. The hippocampus in status epilepticus: demonstration of signal intensity and morphologic changes with sequential fast spin-echo MR imaging. *Radiology* 1995;194:249-256
 24. Chan S, Chin SSM, Kartha K, et al. Reversible signal abnormalities in the hippocampus and neocortex after prolonged seizures. *AJNR Am J Neuroradiol* 1996;17:1725-1731
 25. Wieshmann UD, Woernann FG, Lemieux L, et al. Development of hippocampal atrophy: a serial magnetic resonance imaging study in a patient who developed epilepsy after generalized status epilepticus. *Epilepsia* 1997;38:1238-1241
 26. Nohria V, Lee N, Tien RD, et al. Magnetic resonance imaging evidence of hippocampal sclerosis in progression: a case report. *Epilepsia* 1994;35:1332-1336
 27. Corsellis JA, Bruton CJ. Neuropathology of status epilepticus in humans. *Adv Neurol* 1983;34:129-139
 28. Falconer MA, Serafetinides E, Corsellis JA. Etiology and pathogenesis of temporal lobe epilepsy. *Archs Neurol* 1964;10:233-248
 29. Ingvar M, Morgan PF, Auer RN. The nature and timing of excitotoxic neuronal necrosis in the cerebral cortex, hippocampus and thalamus due to flurothyl-induced status epilepticus. *Acta Neuropathol (Berl)* 1988;75:362-369
 30. Bouillere V, Ridoux V, Depaulis A, Marescaux C, Nehlig A, Salle G. Recurrent seizures and hippocampal sclerosis following intrahippocampal kainate injection in adult mice: electroencephalography, histopathology and synaptic reorganization similar to mesial temporal lobe epilepsy. *Neuroscience* 1999;89:717-729
 31. Sutula TP. Experimental models of temporal lobe epilepsy: new insights from the study of kindling and synaptic reorganization. *Epilepsia* 1990;31:S45-S54
 32. Betram EH, Lothman EW, Lenn NJ. The hippocampus in experimental chronic epilepsy: a morphometric analysis. *Ann Neurol* 1990;27:43-48
 33. Castiglioni AJ, Peterson SL, Sanabria EL, Tiffany CE. Structural changes in astrocytes induced by seizures in a model of temporal lobe epilepsy. *J Neurosci Res* 1990;26:334-341